

Renormalization group equation improved analysis of $B \rightarrow \pi$ form factors from Light-Cone Sum Rules

Yue-Long Shen^a, Yan-Bing Wei^b, Cai-Dian Lü^b

^a*College of Information Science and Engineering, Ocean University of China, Qingdao, Shandong 266100, P.R. China*

^b*Institute of High Energy Physics, CAS, P.O. Box 918(4), Beijing 100049, P.R. China*

ABSTRACT: Within the framework of B -meson light-cone sum rules, we compute the one-loop level QCD corrections to $B \rightarrow \pi$ transition form factors at small q^2 region, in implementation of a complete renormalization group equation evolution. To solve the renormalization group equations, we work at the “dual” space where the anomalous dimensions of the jet function and the light-cone distribution amplitudes are diagonal. With the complete renormalization group equation evolution, the form factors are almost independent of the factorization scale, which is shown numerically. We also extrapolate the results of the form factors to the whole q^2 region, and compare their behavior with other studies.

KEYWORDS: form factors, resummation, light-cone sum rules.

Contents

1. INTRODUCTION	1
2. THE $B \rightarrow \pi$ FORM FACTORS WITH B-MESON LCSRs	3
2.1 NLO corrections to the correlation functions	4
2.2 RGE improved factorization formula	7
2.3 Sum rules of $B \rightarrow \pi$ form factors	10
3. NUMERICAL ANALYSIS	12
4. CONCLUSION AND DISCUSSION	17
A. Jet function in the dual space	19
B. Dispersion integrals	20

1. INTRODUCTION

The knowledge of heavy-to-light transition form factors is of great importance because it can help us to determine CKM parameters, and to explore strong dynamics. In this paper we will concentrate on the $B \rightarrow \pi$ form factors which are closely related to the CKM matrix element $|V_{ub}|$. Usually they are regarded as dominated by long distance QCD dynamics, which can be computed only with the non-perturbative methods, such as Lattice QCD, (Light-Cone) QCD Sum Rules, et al. Light-cone sum rules (LCSR) with pion light-cone distribution amplitudes (LCDAs) has been studied extensively [1, 2, 3]. In this paper, we will employ LCSR with B -meson LCDAs [4, 5, 6, 7] to calculate $B \rightarrow \pi$ transition form factors. The B -meson LCSR has recently been extended to NLO accuracy in α_s expansion [8] for the vector form factors $f_{B\pi}^+(q^2)$, $f_{B\pi}^0(q^2)$ defined below

$$\langle \pi(p) | \bar{u} \gamma_\mu b | \bar{B}(p_B) \rangle = f_{B\pi}^+(q^2) \left[p_B + p - \frac{m_B^2 - m_\pi^2}{q^2} q \right]_\mu + f_{B\pi}^0(q^2) \frac{m_B^2 - m_\pi^2}{q^2} q_\mu, \quad (1.1)$$

where “method of region” [9] is employed to calculate one-loop level corrections to the correlation function at leading power. The results are shown to be consistent with that from SCET sum rules [6, 7], where the correlation function is defined directly using SCET operators [10, 11]. Beside these two vector form factors, we also calculate $B \rightarrow \pi$ tensor form factor $f_{B\pi}^T(q^2)$:

$$\langle \pi(p) | \bar{q} \sigma^{\mu\nu} q_\nu b | B(p_B) \rangle = \frac{i f_{B\pi}^T(q^2)}{m_B + m_\pi} [(p_B + p)_\mu q^2 - (m_B^2 - m_\pi^2) q^\mu], \quad (1.2)$$

which is not computed in [8]. The first step for using method of region is to find out leading regions. It is found that three different momentum modes with the scaling behaviors

$$\begin{aligned} P_\mu &\equiv (n \cdot P, \bar{n} \cdot P, P_\perp), & P_{h,\mu} &\sim \mathcal{O}(1, 1, 1), \\ P_{hc,\mu} &\sim \mathcal{O}(1, \lambda, \lambda^{1/2}), & P_{s,\mu} &\sim \mathcal{O}(\lambda, \lambda, \lambda), \end{aligned} \quad (1.3)$$

can contribute at leading power, where n_μ and \bar{n}_μ are light-cone vectors, satisfying $n^2 = \bar{n}^2 = 0$ and $n \cdot \bar{n} = 2$, and the momentum of fast-moving pion is chosen to be along \bar{n} direction. $P_{h,\mu}$, $P_{hc,\mu}$ and $P_{s,\mu}$ corresponding to the four-momentum of the external b -quark, of the interpolating current of pion and of the light-spectator quark, respectively, will be called hard, hard-collinear and soft modes with $\lambda \sim \Lambda/m_B$. The momentum of interpolating current of pion is chosen to be hard-collinear and $p^2 < 0$ to ensure that the correlation functions can be calculated with light-cone operator product expansion (OPE) [4, 5]. The method of region provides a natural way to perform the factorization of correlation functions because the contributions from different momentum regions are considered individually. It has been shown that the correlation function can be factorized as convolution of the hard function, the jet function and the B -meson distribution amplitudes, which describe the dynamics of hard, hard-collinear and soft region, respectively. This procedure is equivalent to the two-step matching in the soft-collinear effective theory, and the hard (jet) function corresponds to matching coefficient of SCET_I (SCET_{II}) [12, 13].

The correlation functions must be factorization scale independent, thus the scale dependence of the hard function, jet function and B -meson LCDAs should be cancelled, which has been shown at one-loop level [8]. At present, there is still no complete analysis of the RGE evolution for all the relevant functions. In Ref. [8], the RGE evolution of the hard function is performed, while the factorization scale in the jet function is fixed to be about 1.5GeV, which is typical hard-collinear scale. This treatment is reasonable phenomenologically as the hard-collinear scale is not very far from the non-perturbative scale, but on the conceptual side, a complete RGE analysis is necessary. The evolution of the jet function and B -meson wave functions are non-trivial because their anomalous dimension are complicated.

The B -meson LCDAs $\phi_B^-(\omega')$ and $\phi_B^+(\omega')$ are the fundamental inputs in the B -meson LCSR approach. They are defined by the following matrix elements [14, 15]

$$\begin{aligned} &\langle 0 | \bar{d}_\beta(\tau \bar{n}) [\tau \bar{n}, 0] b_\alpha(0) | \bar{B}(p+q) \rangle \\ &= -\frac{i \tilde{f}_B(\mu) m_B}{4} \left\{ \frac{1 + \not{n}}{2} \left[2 \tilde{\phi}_B^+(\tau) + \left(\tilde{\phi}_B^-(\tau) - \tilde{\phi}_B^+(\tau) \right) \not{n} \right] \gamma_5 \right\}_{\alpha\beta}, \end{aligned} \quad (1.4)$$

where $[\tau \bar{n}, 0]$ is the light-cone Wilson line along \bar{n} direction, v and $\tilde{f}_B(\mu)$ are the B -meson velocity vector and decay constant, respectively. The Fourier transformation of $\tilde{\phi}_B^\pm(\tau)$ leads to

$$\phi_B^\pm(\omega') = \int_{-\infty}^{+\infty} \frac{d\tau}{2\pi} e^{i\omega'\tau} \tilde{\phi}_B^\pm(\tau - i0). \quad (1.5)$$

The scale dependence of $\phi_B^\pm(\omega')$ has been extensively studied [16, 17]. They obey the renormalization group equation with the anomalous dimension being Lange-Neubert kernel

[16]. It is less straightforward to express the solution of Lange-Neubert evolution equation in the momentum space. With the eigenfunction of Lange-Neubert kernel found in [17], the evolution equation can be diagonalized and readily solved. Because the scale dependence of the jet function should be partly cancelled by that of the B -meson LCDAs, then the evolution equation of the jet function can be simplified following the same way.

There are two aims of this paper. The first one is to calculate the tensor form factor $f_{B\pi}^T$ in Eq. (1.1) up to one-loop level using B -meson LCSR, which is not considered in [8]. The second one is to carry out a complete RGE analysis of the hard function, jet function and B -meson LCDAs up to two-loop anomalous dimensions level. The remainder of this paper is organized as follows. In section 2 we will provide the analytical expressions of the three $B \rightarrow \pi$ form factors with complete RGE evolution effect. Firstly we briefly review the approach of NLO calculation of $B \rightarrow \pi$ form factors and give the analytical result of the tensor form factor. Then RGE evolution of the correlation functions is shown in detail. At last we obtain the sum rules of the three form factors. In section 3 we turn to the numerical analysis. The concluding discussions are presented in section 4. The Appendix includes two parts, the jet function in the “dual” space and the dispersion integrals used in the sum rules.

2. THE $B \rightarrow \pi$ FORM FACTORS WITH B-MESON LCSRs

The sum rules of the $B \rightarrow \pi$ transition processes can be computed from the following correlation functions

$$\Pi^\mu(p, q) = i \int d^4x e^{ip \cdot x} \langle 0 | T \{ \bar{d}(x) \not{q} \gamma_5 u(x), \bar{u}(0) \Gamma^\mu b(0) \} | \bar{B}(P_B) \rangle, \quad (2.1)$$

with $\Gamma^\mu = \gamma^\mu (\sigma^{\mu\nu} q_\nu)$ for vector (tensor) form factors. The vector form factors have been studied in detail up to $\mathcal{O}(\alpha_s)$ order. Following the same approach we will compute the tensor form factor in the first part of this section. The correlation function of the tensor current can be reduced as $\Pi_\mu(p, q) = \Pi_T(n \cdot p, \bar{n} \cdot p) \epsilon^{\mu\nu} q_\nu$, where $\epsilon^{\mu\nu} = (n^\mu \bar{n}^\nu - \bar{n}^\mu n^\nu)/2$. At deep Euclidean region (in our case $\bar{n} \cdot p < 0$ and $\bar{n} \cdot p \sim \mathcal{O}(\Lambda)$), this correlation function can be calculated from light-cone OPE. At tree level the results read

$$\Pi_T(n \cdot p, \bar{n} \cdot p) = \tilde{f}_B(\mu) m_B \int_0^\infty d\omega' \frac{\phi_B^-(\omega')}{\omega' - \bar{n} \cdot p - i0} + \mathcal{O}(\alpha_s). \quad (2.2)$$

Factorization of $\Pi_\mu(n \cdot p, \bar{n} \cdot p)$ at tree level is straightforward due to the absence of infrared (soft) divergences, i.e.,

$$\Pi_{\mu, b\bar{d}}^{(0)}(n \cdot p, \bar{n} \cdot p) = \int d\omega' T_{\alpha\beta}^{(0)}(n \cdot p, \bar{n} \cdot p, \omega') \Phi_{b\bar{d}}^{(0)\alpha\beta}(\omega'), \quad (2.3)$$

where the superscript (0) indicates the tree level. The leading-order hard-scattering kernel is given by

$$T_{\alpha\beta}^{(0)}(n \cdot p, \bar{n} \cdot p, \omega') = \frac{i}{2} \frac{1}{\bar{n} \cdot p - \omega' + i0} [\not{n} \gamma_5 \not{\bar{n}} \sigma_{\mu\nu} q^\nu]_{\alpha\beta}, \quad (2.4)$$

and the tree-level B -meson DA reads

$$\Phi_{b\bar{d}}^{(0)\alpha\beta}(\omega') = \delta(\bar{n} \cdot k - \omega') \bar{d}_\beta(k) b_\alpha(p_B - k). \quad (2.5)$$

The correlation function can also be expressed in terms of the $B \rightarrow \pi$ tensor form factor and pion decay constant, by inserting the complete set of hadron states with the same quantum number as pion

$$\Pi_T(p, q) = \frac{i(n \cdot p)^2 f_\pi f_{B\pi}^T(q^2)}{2(m_\pi^2 - p^2)} + \int_{\omega_s}^{\infty} d\omega \frac{\rho_h(\omega)}{\omega - \bar{n} \cdot p - i\epsilon}. \quad (2.6)$$

The first term of the right hand of Eq. (2.6) denotes the pion contribution, and the second term of which denotes excited states and continuum contributions. The form factor can be extracted by matching the partonic and the hadronic representation of the correlation function. After performing Borel transformation which can suppress the contribution from higher states, we obtain the sum rules for the tensor form factor at leading order

$$f_{B\pi}^T(q^2) = \frac{\tilde{f}_B(m_B + m_\pi)}{n \cdot p f_\pi} e^{m_\pi^2/(n \cdot p \omega_M)} \int_0^{\omega_s} d\omega e^{-\omega/\omega_M} \phi_-^B(\omega). \quad (2.7)$$

Compared with the sum rules of the vector form factors, it obeys the following form factor relations originated from the spin symmetry [15, 18],

$$f_{B\pi}^+(q^2) = \frac{m_B}{n \cdot p} f_{B\pi}^0(q^2) = \frac{m_B}{m_B + m_\pi} f_{B\pi}^T(q^2). \quad (2.8)$$

2.1 NLO corrections to the correlation functions

The method to compute one-loop corrections to the correlation functions (2.1) has been introduced in [8]. The diagrammatic factorization method [19] is adopted in which the hard-scattering kernel at $\mathcal{O}(\alpha_s)$ is determined by the matching condition

$$\Phi_{b\bar{d}}^{(0)} \otimes T^{(1)} = \Pi_{\mu, b\bar{d}}^{(1)} - \Phi_{b\bar{d}}^{(1)} \otimes T^{(0)}, \quad (2.9)$$

where the first and second terms in the right hand side correspond to the full theory diagrams (Fig. 1) and effective diagrams (Fig. 2). It has been proved that soft dynamics are completely cancelled between these two terms, thus the hard-scattering kernel T contains the contributions only from hard and/or hard-collinear regions at leading power in Λ/m_b . In addition, the collinear divergence is also shown to be absent in the correlation function. In the following we give a brief introduction to the calculation of next-to-leading-order corrections to $\Pi_T(n \cdot p, \mu)$ with method of region. $\Pi_T(n \cdot p, \mu)$ differs from $\Pi(n \cdot p, \mu)$ and $\tilde{\Pi}(n \cdot p, \mu)$ only due to the spin structure of the weak current, it is evident that the result of Fig. 1(c) can be found in [8].

The weak vertex diagram Fig. 1(a) contains leading contribution from hard, hard-collinear and soft regions. Due to the cancellation of soft region contribution between the full and effective diagrams, we only consider the hard and hard-collinear regions. The hard contribution with the loop momentum $l \sim m_b$, is written as

$$\begin{aligned} \Pi_{T,weak}^{(1),h} = & -\frac{2g_s^2 C_F \tilde{f}_B(\mu) m_B}{\bar{n} \cdot p - \omega} \int \frac{d^D l}{(2\pi)^D} \frac{\phi_{b\bar{d}}^-(\omega)}{[l^2 + n \cdot p \bar{n} \cdot l + i0][l^2 + 2m_b v \cdot l + i0][l^2 + i0]} \\ & \times [m_b n \cdot (p + l) + n \cdot p \bar{n} \cdot l + \epsilon(n \cdot l \bar{n} \cdot l - l_\perp^2)]. \end{aligned} \quad (2.10)$$

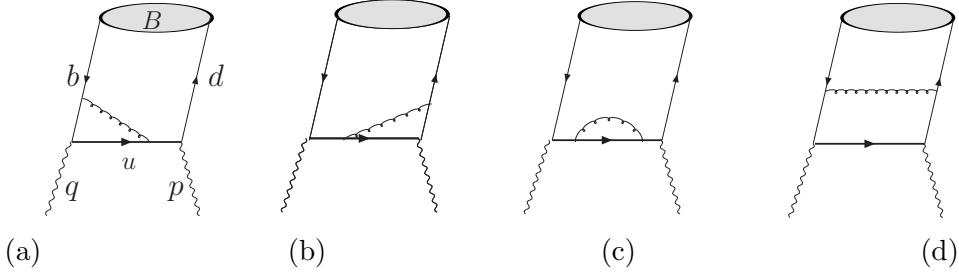


Figure 1: Diagrammatic representation of the correlation function $\Pi_\mu(n \cdot p, \bar{n} \cdot p)$ at $\mathcal{O}(\alpha_s)$.

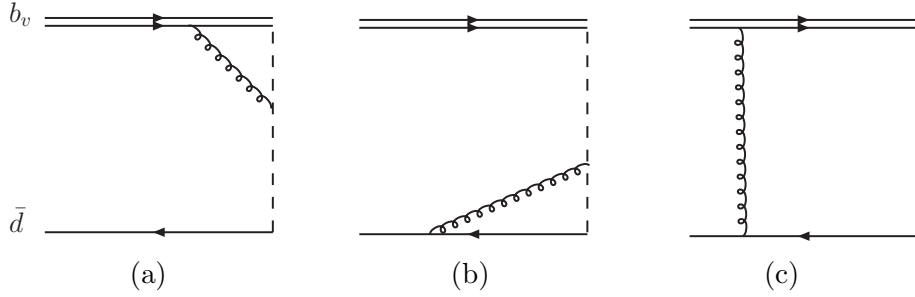


Figure 2: One-loop diagrams for the B -meson DA $\Phi_{b\bar{u}}^{\alpha\beta}(\omega')$.

With the help of the appendix of Ref. [8], the integral result reads

$$\begin{aligned} \Pi_{T,weak}^{(1),h} = & \frac{i\alpha_s C_F}{4\pi} \tilde{f}_B(\mu) m_B \frac{\phi_{b\bar{d}}^-(\omega)}{\bar{n} \cdot p - \omega} \left[\frac{1}{\epsilon^2} + \frac{2}{\epsilon} \left(\ln \frac{\mu}{n \cdot p} + 1 \right) + 2 \ln^2 \frac{\mu}{n \cdot p} \right. \\ & \left. + 4 \ln \frac{\mu}{m_b} - \ln^2 r - 2 \text{Li}_2 \left(-\frac{\bar{r}}{r} \right) - \frac{4r-2}{r-1} \ln r + \frac{\pi^2}{12} + 4 \right], \end{aligned} \quad (2.11)$$

where $r = -n \cdot p/m_B$. Compared with weak vertex diagram induced by the vector current, an additional ultraviolet (UV) divergence term $(\frac{1}{\epsilon} + 2 \ln \frac{\mu}{m_b})$ appears. This new UV divergence arises from the operator renormalization of the weak tensor current. The renormalization scale related to this divergence is different from the factorization scale, and a detailed discussion on this problem will be made in the next section. For the hard-collinear region we have

$$\begin{aligned} \Pi_{T,weak}^{(1),hc} = & \frac{g_s^2 C_F \tilde{f}_B(\mu) m_B}{\omega - \bar{n} \cdot p} \int \frac{d^D l}{(2\pi)^D} \frac{\phi_{b\bar{d}}^-[2m_b n \cdot (p+l)]}{[n \cdot (p+l) \bar{n} \cdot (p-k+l) + l_\perp^2 + i0]} \\ & \times \frac{1}{[m_b n \cdot l + i0][l^2 + i0]}, \end{aligned} \quad (2.12)$$

which is the same with the vector current case, indicating the universality of the jet function.

For the pion vertex and box diagrams, the hard region is suppressed Ref. [8], thus only

the hard-collinear region is essential. The results can be written by

$$\begin{aligned}
\Pi_{T,pion}^{(1)} &= \frac{i\alpha_s C_F}{4\pi} \tilde{f}_B(\mu) m_B \left\{ \frac{\phi_{b\bar{d}}^-(\omega)}{\bar{n} \cdot p - \omega} \frac{1}{2} \left[\left(\frac{1}{\epsilon} + \ln \left(-\frac{\mu^2}{p^2} \right) \right) \left(\frac{2\bar{n} \cdot p}{\omega} \ln \frac{\bar{n} \cdot p - \omega}{\bar{n} \cdot p} + 1 \right) \right. \right. \\
&\quad \left. \left. - \frac{\bar{n} \cdot p}{\omega} \ln \frac{\bar{n} \cdot p - \omega}{\bar{n} \cdot p} \left(\ln \frac{\bar{n} \cdot p - \omega}{\bar{n} \cdot p} + \frac{2\omega}{\bar{n} \cdot p} - 4 \right) + 3 \right] \right. \\
&\quad \left. + \frac{\phi_{b\bar{d}}^+(\omega)}{\bar{n} \cdot p - \omega} \frac{(1+\eta) \ln(1+\eta)}{2\eta} \right\} \\
\Pi_{T,box}^{(1)} &= -\frac{i\alpha_s C_F \tilde{f}_B(\mu) m_B}{4\pi} \frac{\phi_{b\bar{d}}^-(\omega)}{\omega} \ln(1+\eta) \left[\frac{1}{\epsilon} + \ln \frac{\mu^2}{n \cdot p (\omega - \bar{n} \cdot p)} \right. \\
&\quad \left. + \frac{1}{2} \ln(1+\eta) + 1 \right], \tag{2.13}
\end{aligned}$$

where $\eta = -\omega/\bar{n} \cdot p$. Two remarks are made here:

- In the pion vertex diagram, the third term in the B -meson projector [7]

$$\begin{aligned}
M_{\beta\alpha} &= -\frac{i\tilde{f}_B(\mu) m_B}{4} \\
&\quad \times \left\{ \frac{1+\not{p}}{2} \left[\phi_B^+(\omega') \not{\epsilon} + \phi_B^-(\omega') \not{\bar{\epsilon}} - \frac{2\omega'}{D-2} \phi_B^-(\omega') \gamma_\perp^\rho \frac{\partial}{\partial k_\perp^\rho} \right] \gamma_5 \right\}_{\alpha\beta} \tag{2.14}
\end{aligned}$$

must be included because the transverse momentum dependent term contributes at leading power.

- The universality of jet function seems not holding for this two diagrams, due to different $\phi_B^+(\omega')$ terms from the vector current case. But when these two diagrams are summed up, the universality is recovered .

Including all the contributions from leading regions, we arrive at the factorization formula of the correlation function:

$$\begin{aligned}
\Pi_T(n \cdot p, \mu) &= \tilde{f}_B(\mu) m_B \sum_{k=\pm} C^{(k)}(n \cdot p, \mu) \\
&\quad \times \int_0^\infty \frac{d\omega}{\omega - \bar{n} \cdot p} J^{(k)} \left(\frac{\mu^2}{n \cdot p \omega}, \frac{\omega}{\bar{n} \cdot p} \right) \phi_B^{(k)}(\omega, \mu), \tag{2.15}
\end{aligned}$$

where the hard functions are written

$$\begin{aligned}
C^{(+)} &= 1, \\
C^{(-)} &= 1 - \frac{\alpha_s C_F}{4\pi} \left[2 \ln^2 \frac{\mu}{n \cdot p} + 7 \ln \frac{\mu}{m_b} - \ln^2 r - 2 \text{Li}_2 \left(-\frac{\bar{r}}{r} \right) \right. \\
&\quad \left. - \frac{4r-2}{r-1} \ln r - \frac{\pi^2}{12} + 6 \right]. \tag{2.16}
\end{aligned}$$

The jet functions integrate the dynamics from the hard-collinear region

$$J^{(+)} = \frac{\alpha_s C_F}{4\pi} (1+\eta) \ln(1+\eta),$$

$$J^{(-)} = 1 + \frac{\alpha_s C_F}{4\pi} \left[\ln^2 \frac{\mu^2}{n \cdot p(\omega - \bar{n} \cdot p)} - 2 \ln \frac{\bar{n} \cdot p - \omega}{\bar{n} \cdot p} \ln \frac{\mu^2}{n \cdot p(\omega - \bar{n} \cdot p)} - \ln^2 \frac{\bar{n} \cdot p - \omega}{\bar{n} \cdot p} - \left(1 + \frac{2\bar{n} \cdot p}{\omega} \right) \ln \frac{\bar{n} \cdot p - \omega}{\bar{n} \cdot p} - \frac{\pi^2}{6} - 1 \right]. \quad (2.17)$$

2.2 RGE improved factorization formula

Large logarithmic terms such as $\ln^2 \frac{\mu}{m_b}$ and $\ln \frac{\mu}{m_b}$ appear in the hard and jet functions, when the factorization scale μ is much smaller than m_B . They need to be resummed using renormalization group equation method. Because $\Pi_T(n \cdot p)$ includes additional operator renormalization, it is most suitable object to illustrate the procedure of the RGE evolution, and all the results can be easily generalized to $\Pi(n \cdot p)$ and $\tilde{\Pi}(n \cdot p)$.

Firstly we need to distinguish renormalization scale ν and factorization scale μ in the hard function Eq. (2.16). Following [20] the hard coefficient can be decomposed as

$$C^{(-)}(n \cdot p, \mu, \nu) = C^{(-)}(n \cdot p, \mu) + \delta C^{(-)}(n \cdot p, \mu, \nu), \quad (2.18)$$

where the second term is related to the well-known anomalous dimension of the tensor current :

$$\delta C^{(-)}(n \cdot p, \mu, \nu) = -\frac{\alpha_s C_F}{2\pi} \ln \frac{\nu}{\mu}. \quad (2.19)$$

The explicit expression of the hard function is then written as

$$C^{(-)}(n \cdot p, \mu, \nu) = 1 - \frac{\alpha_s C_F}{4\pi} \left[2 \ln \frac{\nu}{m_B} + 2 \ln^2 \frac{\mu}{m_B} - (4 \ln r - 5) \ln \frac{\mu}{m_B} + 2 \ln^2 r + 2 \text{Li}_2(\bar{r}) - \frac{4r-2}{r-1} \ln r + \frac{\pi^2}{12} + 6 \right]. \quad (2.20)$$

The RG equations governing renormalization and factorization scale evolution are given by

$$\begin{aligned} \frac{d}{d \ln \mu} C^{(-)}(n \cdot p, \mu, \nu) &= \Gamma_C(\mu) C^{(-)}(n \cdot p, \mu), \\ \frac{d}{d \ln \nu} C^{(-)}(n \cdot p, \mu, \nu) &= \gamma_T(\alpha_s) C^{(-)}(n \cdot p, \mu, \nu), \end{aligned} \quad (2.21)$$

where the anomalous dimension for the hard function is

$$\Gamma_C(\mu) = -\Gamma_{\text{cusp}}(\alpha_s) \ln \frac{\mu}{n \cdot p} + \gamma_h(\alpha_s). \quad (2.22)$$

The cusp anomalous dimension $\Gamma_{\text{cusp}}(\alpha_s)$ should be expanded to 3-loop level ,

$$\Gamma_{\text{cusp}}(\alpha_s) = \frac{\alpha_s C_F}{4\pi} \left[\Gamma_{\text{cusp}}^{(0)} + \left(\frac{\alpha_s}{4\pi} \right) \Gamma_{\text{cusp}}^{(1)} + \left(\frac{\alpha_s}{4\pi} \right)^2 \Gamma_{\text{cusp}}^{(2)} + \dots \right], \quad (2.23)$$

and the anomalous dimension γ_h and γ_T need to be expanded to two-loop level:

$$\begin{aligned} \gamma_h(\alpha_s) &= \frac{\alpha_s C_F}{4\pi} \left[\gamma_h^{(0)} + \left(\frac{\alpha_s}{4\pi} \right) \gamma_h^{(1)} + \dots \right], \\ \gamma_T(\alpha_s) &= \frac{\alpha_s C_F}{4\pi} \left[-2 + \frac{\alpha_s}{4\pi} \left(19C_F - \frac{257}{9}C_A + \frac{52}{9}(n_l + 1)T_F \right) + \dots \right]. \end{aligned} \quad (2.24)$$

Solving renormalization scale evolution equation in Eq. (2.21), it yields:

$$C^{(-)}(n \cdot p, \mu, \nu) = e^{\int_{m_b}^{\nu} \frac{d\nu'}{\nu'} \gamma_T(\alpha_s)} C^{(-)}(n \cdot p, \mu, m_b), \quad (2.25)$$

Note that ν dependence of the form factor must be cancelled by the Wilson coefficient of the tensor current. For phenomenological applications, it can be fixed at $\nu = m_b$, then this kernel is reduced to 1. To make the correlation function scale independent, the Wilson coefficient of the tensor current should be evolved to m_b scale. The solution to the first equation in Eq. (2.21), which resums large logarithmic terms $\ln(\mu/\mu_{h1})$ and $\ln^2(\mu/\mu_{h1})$, with the hard scale $\mu_{h1} \sim n \cdot p$, can be written by

$$C^{(-)}(n \cdot p, \mu) = U_1(n \cdot p, \mu_{h1}, \mu) C^{(-)}(n \cdot p, \mu_{h1}), \quad (2.26)$$

where the specific expression for $U_1(n \cdot p, \mu_{h1}, \mu)$ can be found in the appendix of [21].

The RGEs for the jet function and the wave function have the following form

$$\begin{aligned} \frac{d}{d \ln \mu} J^{(-)} \left(\frac{\mu^2}{n \cdot p \omega}, \frac{\omega}{\bar{n} \cdot p} \right) &= \left[\Gamma_{\text{cusp}}(\alpha_s) \ln \frac{\mu^2}{n \cdot p \omega} \right] J^{(-)} \left(\frac{\mu^2}{n \cdot p \omega}, \frac{\omega}{\bar{n} \cdot p} \right) \\ &+ \int_0^\infty d\omega' \omega \Gamma(\omega, \omega', \mu) J^{(-)} \left(\frac{\mu^2}{n \cdot p \omega'}, \frac{\omega'}{\bar{n} \cdot p} \right), \end{aligned} \quad (2.27)$$

$$\begin{aligned} \frac{d}{d \ln \mu} \phi_B^-(\omega, \mu) &= - \left[\Gamma_{\text{cusp}}(\alpha_s) \ln \frac{\mu}{\omega} + \gamma_+(\alpha_s) \right] \phi_B^-(\omega, \mu) \\ &- \int_0^\infty d\omega' \omega \Gamma(\omega, \omega', \mu) \phi_B^-(\omega', \mu), \end{aligned} \quad (2.28)$$

where the evolution kernel is not diagonal, thus it is more involved to solve the above RGEs in the momentum space. An alternative method is suggested in [17], where the evolution equation is translated into the “dual” space and the LN kernel is diagonalized. It is found in [22] that the basis of the dual space is actually the eigenfunction of the generator of special conformal transformations. The specific form of the transformation can be written by:

$$\rho_B^-(\omega', \mu) = \int_0^\infty \frac{d\omega}{\omega'} J_0(2\sqrt{\frac{\omega}{\omega'}}) \phi_B^-(\omega, \mu), \quad (2.29)$$

where the dual space function ρ_B^- satisfies a simpler RG equation

$$\frac{d}{d \ln \mu} \rho_B^-(\omega', \mu) = \Gamma_\rho(\mu) \rho_B^-(\omega', \mu), \quad (2.30)$$

with $\Gamma_\rho(\mu) = -\Gamma_{\text{cusp}}(\alpha_s) \ln \frac{\mu}{\hat{\omega}'} - \gamma_+(\alpha_s)$, $\hat{\omega}' = e^{-2\gamma_E} \omega'$. In the dual space it is straightforward to write down

$$\rho_B^-(\omega', \mu) = e^{V(\mu, \mu_0)} \left(\frac{\mu_0}{\hat{\omega}'} \right)^{-g(\mu, \mu_0)} \rho_B^-(\omega', \mu_0) \quad (2.31)$$

where

$$\begin{aligned} V(\mu, \mu_0) &= - \int_{\alpha_s(\mu_0)}^{\alpha_s(\mu)} \frac{d\alpha}{\beta(\alpha)} \left[\Gamma_{\text{cusp}}(\alpha) \int_{\alpha_s(\mu_0)}^{\alpha} \frac{d\alpha'}{\beta(\alpha')} + \gamma_+(\alpha) \right] \\ g(\mu, \mu_0) &= - \int_{\alpha_s(\mu_0)}^{\alpha_s(\mu)} d\alpha \frac{\Gamma_{\text{cusp}}(\alpha)}{\beta(\alpha)}. \end{aligned} \quad (2.32)$$

Using the orthogonality of the Bessel function, we can express $\phi_B^-(\omega, \mu)$ in terms of $\rho_B^-(\omega', \mu)$:

$$\phi_B^-(\omega, \mu) = \int_0^\infty \frac{d\omega'}{\omega'} J_0(2\sqrt{\frac{\omega}{\omega'}}) \rho_B^-(\omega', \mu), \quad (2.33)$$

which can be substituted into Eq. (2.15), leading to the factorization formula of the correlation function in the dual space,

$$\begin{aligned} \Pi_T(\mu, n \cdot p) &= \tilde{f}_B(\mu) m_B \sum_{k=\pm} C^{(k)}(n \cdot p, \mu) \\ &\times \int_0^\infty \frac{d\omega'}{\omega'} j^{(k)}(\hat{\omega}', \mu) \rho_B^{(k)}(\omega', \mu), \end{aligned} \quad (2.34)$$

where $j^{(k)}(\hat{\omega}', \mu)$ is the jet function in the dual space. The explicit expression of $j^+(\hat{\omega}', \mu)$ term is not provided because the terms containing $J^+(\frac{\omega}{n \cdot p})$ are computed in momentum space (see the first comment in next subsection). We may rewrite $j^-(\hat{\omega}', \mu)$ as $j(\hat{\omega}', \mu)$, which satisfy the following evolution equation

$$\frac{d}{d \ln \mu} j(\hat{\omega}', \mu) = \Gamma_j(\mu) j(\hat{\omega}', \mu). \quad (2.35)$$

The scale independence of the correlation function results in the relation

$$\Gamma_j(\mu) = -\Gamma_C(\mu) - \Gamma_\rho(\mu) - \tilde{\gamma}(\alpha_s(\mu)), \quad (2.36)$$

where $\tilde{\gamma}(\alpha_s)$ is the anomalous dimension of the decay constant $\tilde{f}(\mu)$. The RG equation of $\tilde{f}_B(\mu)$ at two-loop order is given by

$$\frac{d}{d \ln \mu} \tilde{f}_B(\mu) = \tilde{\gamma}(\alpha_s) \tilde{f}_B(\mu), \quad (2.37)$$

with

$$\begin{aligned} \tilde{\gamma}(\alpha_s) &= \frac{\alpha_s C_F}{4\pi} \left[\tilde{\gamma}^{(0)} + \left(\frac{\alpha_s}{4\pi} \right) \tilde{\gamma}^{(1)} + \dots \right], \\ \tilde{\gamma}^{(0)} &= 3, \quad \tilde{\gamma}^{(1)} = \frac{127}{6} + \frac{14\pi^2}{9} - \frac{5}{3} n_f, \end{aligned} \quad (2.38)$$

where $n_f = 4$ is the number of light quark flavors. Solving this RG equation yields

$$\begin{aligned} U_2(\mu_{h2}, \mu) &= \text{Exp} \left[\int_{\alpha_s(\mu_{h2})}^{\alpha_s(\mu)} d\alpha_s \frac{\tilde{\gamma}(\alpha_s)}{\beta(\alpha_s)} \right] \\ &= z^{-\frac{\tilde{\gamma}_0}{2\beta_0} C_F} \left[1 + \frac{\alpha_s(\mu_{h2}) C_F}{4\pi} \left(\frac{\tilde{\gamma}^{(1)}}{2\beta_0} - \frac{\tilde{\gamma}^{(0)} \beta_1}{2\beta_0^2} \right) (1-z) + \mathcal{O}(\alpha_s^2) \right], \end{aligned} \quad (2.39)$$

with $z = \alpha_s(\mu)/\alpha_s(\mu_{h2})$.

The anomalous dimensions must be expressed as

$$\Gamma_j = \Gamma_{\text{cusp}}(\alpha_s) \ln \frac{\mu^2}{n \cdot p \hat{\omega}'} + \left(\frac{\alpha_s}{4\pi} \right)^2 C_F \gamma_{hc}(\alpha_s), \quad (2.40)$$

with $\gamma_{hc}(\alpha_s) = \frac{\alpha_s C_F}{4\pi} [\gamma_{hc}^{(0)} + (\frac{\alpha_s}{4\pi}) \gamma_{hc}^{(1)} + \dots]$, at one-loop level $\gamma_{hc}^{(0)} = 0$, while there is no result for $\gamma_{hc}^{(1)}$ so far. It may be derived from the relation $\gamma_{hc}^{(1)} = -\gamma_h^{(1)} + \gamma_+^{(1)} - \tilde{\gamma}^{(1)}$, where $\gamma_h^{(1)}$ and $\tilde{\gamma}^{(1)}$ have been calculated up to two-loop level, but $\gamma_+^{(1)}$ is also unknown yet, which prevents us from performing a totally complete evolution of the correlation functions up to two-loop level. In our numerical calculations, we assume $\gamma_{hc}^{(1)} = 0$, and it has been checked numerically that the uncertainty from this parameter is small. The evolution function of $j(\hat{\omega}', \mu)$ can be obtained easily

$$j(\hat{\omega}', \mu) = e^{-2V_{hc}(\mu, \mu_{hc})} \left(\frac{\mu_{hc}^2}{\hat{\omega}' \bar{n} \cdot p} \right)^{g(\mu, \mu_{hc})} j(\hat{\omega}', \mu_{hc}), \quad (2.41)$$

The specific expression for $j(\hat{\omega}', \mu_{hc})$ is given by:

$$\begin{aligned} j(\hat{\omega}', \mu_{hc}) &= 2K_0 \left(2\sqrt{\frac{1}{\eta'}} \right) \left\{ 1 + \frac{\alpha_s C_F}{4\pi} \left[\ln^2 \frac{\mu_{hc}^2}{-p^2} - \frac{\pi^2}{6} - 1 - \frac{1}{2} \ln \hat{\eta}' (4 \ln \frac{\mu_{hc}^2}{-p^2} + 3) \right. \right. \\ &\quad \left. \left. + \frac{1}{4} \ln^2 \hat{\eta}' - \frac{1}{6} \pi^2 \right] \right\} + \frac{\alpha_s C_F}{2\pi} K_0^{(2,0)} \left(2\sqrt{\frac{1}{\eta'}} \right) \\ &\quad + \frac{\alpha_s C_F}{\pi} \int_{2\sqrt{\frac{1}{\eta'}}}^{\infty} \frac{d\beta}{\beta} K_0(\beta), \end{aligned} \quad (2.42)$$

where $\hat{\eta}' = e^{-2\gamma_E} \eta' = -\hat{\omega}' / \bar{n} \cdot p$ (the detailed derivation of $j(\hat{\omega}', \mu_{hc})$ is given in Appendix A). We collect the evolution of the hard function, the jet function, the B -meson LCDAs and the B -meson decay constant together, finally obtain the result of RGE evolution

$$\begin{aligned} \Pi_T(\bar{n} \cdot p) &= m_B [U_1(n \cdot p, \mu_{h1}, \mu) U_2(\mu_{h2}, \mu)] \left[\tilde{f}_B(\mu_{h2}) C^{(-)}(n \cdot p, \mu_{h1}) \right] \\ &\quad \times \int_0^{\infty} \frac{d\omega'}{\omega'} U_j(n \cdot p, \mu_{hc}, \mu) j(\hat{\omega}', \mu_{hc}) U_\rho(n \cdot p, \mu_0, \mu) \rho_B^{(-)}(\omega', \mu_0) \\ &\quad + m_B U_2(\mu_{h2}, \mu) \tilde{f}_B(\mu_{h2}) \int_0^{\infty} \frac{d\omega}{\omega - \bar{n} \cdot p} J^{(+)} \left(\frac{\omega}{\bar{n} \cdot p} \right) \phi_B^{(+)}(\omega, \mu), \end{aligned} \quad (2.43)$$

where

$$\begin{aligned} U_j(n \cdot p, \mu_{hc}, \mu) &= e^{-2V_{hc}(\mu, \mu_{hc})} \left(\frac{\mu_{hc}^2}{\hat{\omega}' \bar{n} \cdot p} \right)^{g(\mu, \mu_{hc})}, \\ U_\rho(n \cdot p, \mu_0, \mu) &= e^{V(\mu, \mu_0)} \left(\frac{\mu_0}{\hat{\omega}'} \right)^{-g(\mu, \mu_0)}, \end{aligned} \quad (2.44)$$

2.3 Sum rules of $B \rightarrow \pi$ form factors

Now we are in the position to construct the sum rules for the three $B \rightarrow \pi$ form factors at NLO order. The dispersion integrals used here are collected in the Appendix B. Performing Borel transformation, we can obtain the final results of the $B \rightarrow \pi$ form factors. The tensor form factor reads

$$\begin{aligned} f_\pi e^{-m_\pi^2 n \cdot p / \omega_M^2} f_{B\pi}^T(q^2) &= U_2(\mu_{h2}, \mu) \tilde{f}_B(\mu_{h2}) \int_0^{\omega_s} d\omega e^{-\omega/\omega_M} \left[\phi_{B,eff}^+(\omega) \right. \\ &\quad \left. + U_1(n \cdot p, \mu_{h1}, \mu) C^{(-)}(n \cdot p, \mu_{h1}) \rho_{eff}^-(\omega) \right], \end{aligned} \quad (2.45)$$

where

$$\begin{aligned}
\phi_{B,\text{eff}}^+(\Omega, \mu) &= \frac{\alpha_s C_F}{4\pi} \int_{\Omega}^{\infty} \frac{d\omega}{\omega} \phi_B^+(\omega, \mu) , \\
\rho_{eff}^-(\Omega, \mu) &= \int_0^{\infty} \frac{d\omega'}{\omega'} \left\{ \left[1 + \frac{\alpha_s C_F}{4\pi} \left(\ln^2 \frac{\mu^2}{n \cdot p \Omega} - 2 \ln \frac{\mu^2}{n \cdot p \Omega} \ln \frac{\hat{\omega}'}{\Omega} \right. \right. \right. \\
&\quad \left. \left. + \frac{1}{2} \ln^2 \frac{\hat{\omega}'}{\Omega} - \frac{3}{2} \ln \frac{\hat{\omega}'}{\Omega} + \frac{\pi^2}{2} - 1 \right) \right] J_0 \left(2\sqrt{\frac{\Omega}{\omega'}} \right) \\
&\quad \left. + \frac{\alpha_s C_F}{4\pi} \left(\ln \frac{\hat{\omega}'}{\Omega} + \frac{3}{2} \right) \pi N_0 \left(2\sqrt{\frac{\Omega}{\omega'}} \right) \right. \\
&\quad \left. + \frac{\alpha_s C_F}{2\pi} \left[J_0^{(2,0)} \left(2\sqrt{\frac{\Omega}{\omega'}} \right) + \frac{\Omega}{\omega'^2} F_3(1, 1; 2, 2, 2; -\frac{\Omega}{\omega'}) - \ln \frac{\Omega}{\hat{\omega}'} \right] \right\} \\
&\quad \times U_j(\mu_{hc}, \mu) U_{\rho}(\mu_0, \mu) \rho_B^{(-)}(\omega', \mu_0) , \tag{2.46}
\end{aligned}$$

with ${}_pF_q(a_1 \dots a_p; b_1 \dots b_q; z)$ is the generalized Hypergeometric function. The vector form factors $f_{B\pi}^{+,0}$ are closely related to the tensor form factor

$$\begin{aligned}
&f_{\pi} e^{-m_{\pi}^2/(n \cdot p \omega_M)} \left\{ \frac{n \cdot p}{m_B} f_{B\pi}^+(q^2), f_{B\pi}^0(q^2) \right\} \\
&= \left[U_2(\mu_{h2}, \mu) \tilde{f}_B(\mu_{h2}) \right] \int_0^{\omega_s} d\omega' e^{-\omega'/\omega_M} \left[r \phi_{B,\text{eff}}^+(\omega', \mu) \right. \\
&\quad \left. + \left[U_1(n \cdot p, \mu_{h1}, \mu) \tilde{C}^{(-)}(n \cdot p, \mu_{h1}) \right] \rho_{B,\text{eff}}^-(\omega', \mu) \right. \\
&\quad \left. \pm \frac{n \cdot p - m_B}{m_B} \left(\phi_{B,\text{eff}}^+(\omega', \mu) + C^{(-)}(n \cdot p, \mu) \phi_B^-(\omega', \mu) \right) \right] . \tag{2.47}
\end{aligned}$$

For the above results, several comments are as follows:

- The RGE evolution has only been applied to the $C^{(-)} \cdot J^{(-)} \otimes \phi^{(-)}$ ($\tilde{C}^{(-)} \cdot \tilde{J}^{(-)} \otimes \phi^{(-)}$ terms in the vector form factors), but not to the $C^{(+)} \cdot J^{(+)} \otimes \phi^{(+)}$ term. Since $J^{(+)}$ term begin with the α_s order, when derivative is performed to them with respect to $\ln \mu$, an additional α_s will appear, so that this term cannot contribute at the present order.
- According to the above comment, terms containing $\phi_B^+(\omega)$ is not RGE evolved at the present order, thus the result will not change when the jet function and the B -meson LCDAs are translated to the dual space. It is simpler to keep the expression in momentum space.
- The dispersion integrals in the momentum space is non-trivial for the appearance of both pole and branch-cut, which can be seen in the appendix of [7]. While in the dual space, the jet function in $\rho_{eff}^-(\Omega, \mu)$ can be obtained straightforwardly by the simple replacement $\bar{n} \cdot p \rightarrow \Omega e^{-i\pi}$.

3. NUMERICAL ANALYSIS

In this section we will perform the numerical analysis of the three $B \rightarrow \pi$ form factors with sum rules improved by resummation. To illustrate the effect of RGE evolution, we will employ the same input parameters with [8], where an incomplete evolution scheme is adopted. The B -meson LCDAs serve as fundamental ingredients for the LCSR of the $B \rightarrow \pi$ form factors, but so far there is a very limited knowledge on these LCDAs. Several phenomenological models are suggested in [7, 14, 23], which are employed in the evaluation of the $B \rightarrow \pi$ form factors with B -meson LCSR [8]. The results indicate that different models can give similar results. Here we adopt the following widely-used model,

$$\phi_B^+(\omega, \mu_0) = \frac{\omega}{\omega_0^2} e^{-\omega/\omega_0}. \quad (3.1)$$

Neglecting the contribution from three-particle Fock state, the corresponding expression of $\phi_B^-(\omega, \mu_0)$ for this model is determined with Wandzura-Wilczek approximation [15]

$$\phi_B^-(\omega, \mu_0) = \int_0^1 \frac{d\xi}{\xi} \phi_B^+\left(\frac{\omega}{\xi}, \mu_0\right). \quad (3.2)$$

The parameter ω_0 appears in the above model, is actually the inverse moment of B -meson LCDAs, which is defined below

$$\lambda_B^{-1}(\mu) = \int_0^\infty \frac{d\omega}{\omega} \phi_B^+(\omega, \mu) = \frac{1}{\omega_0}. \quad (3.3)$$

This parameter is closely related to the radiative and non-leptonic B -meson decays, but the experimental data can only give a very rough constraint. In the present work we adopt the seem value with [8], where ω_0 is determined by fixing $f_{B\pi}^+(q^2 = 0) = 0.28 \pm 0.03$ [3].

Because the RGEs of the jet function and B -meson LCDAs are evaluated in the dual space, we need to know the dual expression of ϕ_B^- , which has been given in [17]

$$\rho_B^-(\omega', \mu) = \frac{1}{\omega'} e^{-\omega_0/\omega'}. \quad (3.4)$$

To give a more intuitive picture of the above B -meson LCDA, we plot the ω' dependence diagram in Fig. 3. The dashed line denotes $\rho_B^-(\omega', \mu)$ defined in Eq. (3.4), and the solid line stands for $\rho_{eff}^-(\Omega, \mu)$ in Eq. (2.46), which contains the evolution factors of jet function and B -meson LCDAs. We can observe that after including these factors, large ω' region is manifestly suppressed while small ω' region is enhanced.

Before presenting the numerical results of the form factors, we first show the behavior of the evolution factors of the hard function ($U_1(\mu, \mu_{h1})$), the jet function ($U_j(\mu, \mu_{hc})$), the LCDAs ($U\rho(\mu, \mu_0)$) and the B -meson decay constant ($U_2(\mu, \mu_{h2})$), respectively, in Fig. 4. When plotting this diagram, ω' is fixed at a small value 0.2GeV (this region will give important contribution in the form factors). This choice leads to large logarithmic terms in the evolution kernel of the LCDAs and the jet function, hence the evolution effect of these two parts is significant. The slopes of their curves have different sign, so that the

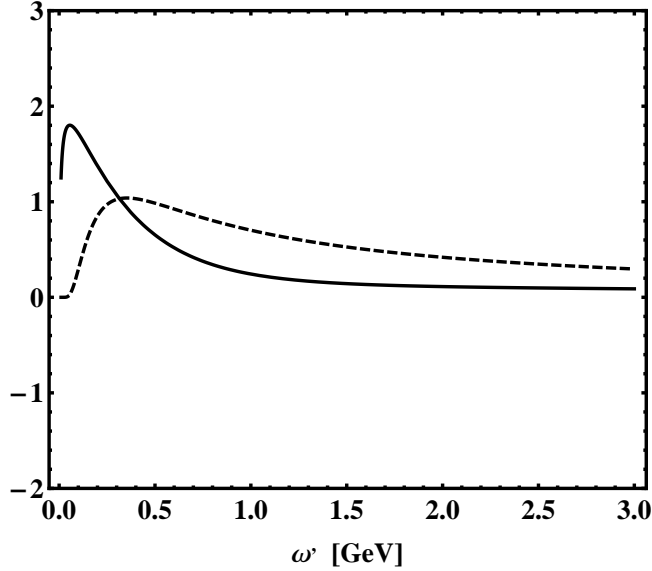


Figure 3: Shape of the wave functions in the dual space. The dashed line stands for the wave functions $\rho_B^-(\omega', \mu)$, and the effective function $\rho_{eff}^-(\Omega, \mu)$ defined in Eq. (2.46) is denoted by the solid line.

cancellation effect is strong which is important to guarantee the scale invariance of the form factors.

In the LCSR approach, the form factors should be insensitive to the Borel mass and the effective threshold. These parameters could be constrained following the conditions in [8], where the contribution from the continuum state should be less than 40% and the rate of change $\frac{\partial \ln f^T(q^2)}{\partial \ln \omega_M} \leq 35\%$. We fix $q^2 = 0$ to study the ω_M and s_0 dependence of the form factors. The above constraints lead to a region $0.24 \leq \omega_M \leq 0.36$ for the tensor form factor (corresponding to $1.0 \leq M^2/\text{GeV} \leq 1.5$), which is consistent with that of the vector form factors [8]. The Borel mass and threshold parameter dependence of the form factors $f^T(0)$ and $f^+(0)$ are plotted in Fig. 5. The obvious platforms indicate the stability of the LCSR predictions.

Now we consider the scale dependence of the form factors. With the complete RGE evolution, it is expected that the scale dependence of our predictions should be very mild. In Fig. 6, the dependence on the factorization scale of the tensor form factor is plotted. Three curves related to different schemes are shown to illustrate the improvement of the RGE evolution. The purple dashed line represents RGE evolution only performed for the hard function and the B-meson decay constant, and it exhibits that the tensor form factor increases with the increasing scale. If an addition evolution of the inverse moment λ_B are included, corresponding to the strategy used in [8], the scale dependence is manifestly suppressed, which can be seen by the black dashed line. While when the complete RGE is

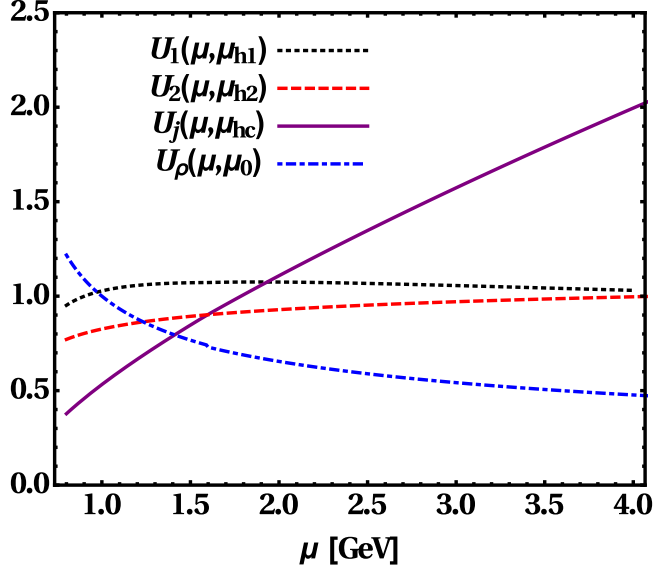


Figure 4: The evolution factors of the hard function, the B-meson decay constant, the jet function and the wave function, which are denoted using black dotted, red dashed, blue dot-dashed and purple solid line, respectively.

adopted, the form factors is almost independent on the energy scale, as shown by the blue solid line.

It has been argued that in the $B \rightarrow \pi$ transitions, the LCSR with B -meson LCDAs can be trusted at $q^2 \leq q_{max}^2 = 8 \text{ GeV}^2$ (see [5] for more detailed discussions). To extrapolate the computed form factors from the LCSR method at large recoil toward large momentum transfer q^2 , we follow the same way with [8], where the z -series parameterization is employed. In this approach, the cut q^2 -plane along the positive real axis is mapped onto the unit disk $|z(q^2, t_0)| < 1$ via the conformal transformation

$$z(q^2, t_0) = \frac{\sqrt{t_+ - q^2} - \sqrt{t_+ - t_0}}{\sqrt{t_+ - q^2} + \sqrt{t_+ - t_0}}, \quad (3.5)$$

where $t_+ = (m_B + m_\pi)^2$ denotes the threshold of continuum states in the $B^*(1^-)$ meson channel. The free parameter $t_0 \in (-\infty, t_+)$ determines the value of q^2 mapped onto the origin in the z plane and can be adjusted to minimize the z interval from mapping the LCSR region $q_{min}^2 \leq q^2 \leq q_{max}^2$ and can be chosen as [3]

$$t_0 = t_+^2 - \sqrt{t_+ - t_-} \sqrt{t_+ - q_{min}^2}, \quad (3.6)$$

with $q_{min}^2 = -6.0 \text{ GeV}^2$ and $t_- \equiv (m_B - m_\pi)^2$.

Employing the z -series expansion and taking into account the threshold t_+ behavior, one can obtain the parametrization of each form factor. The parametrization of the two

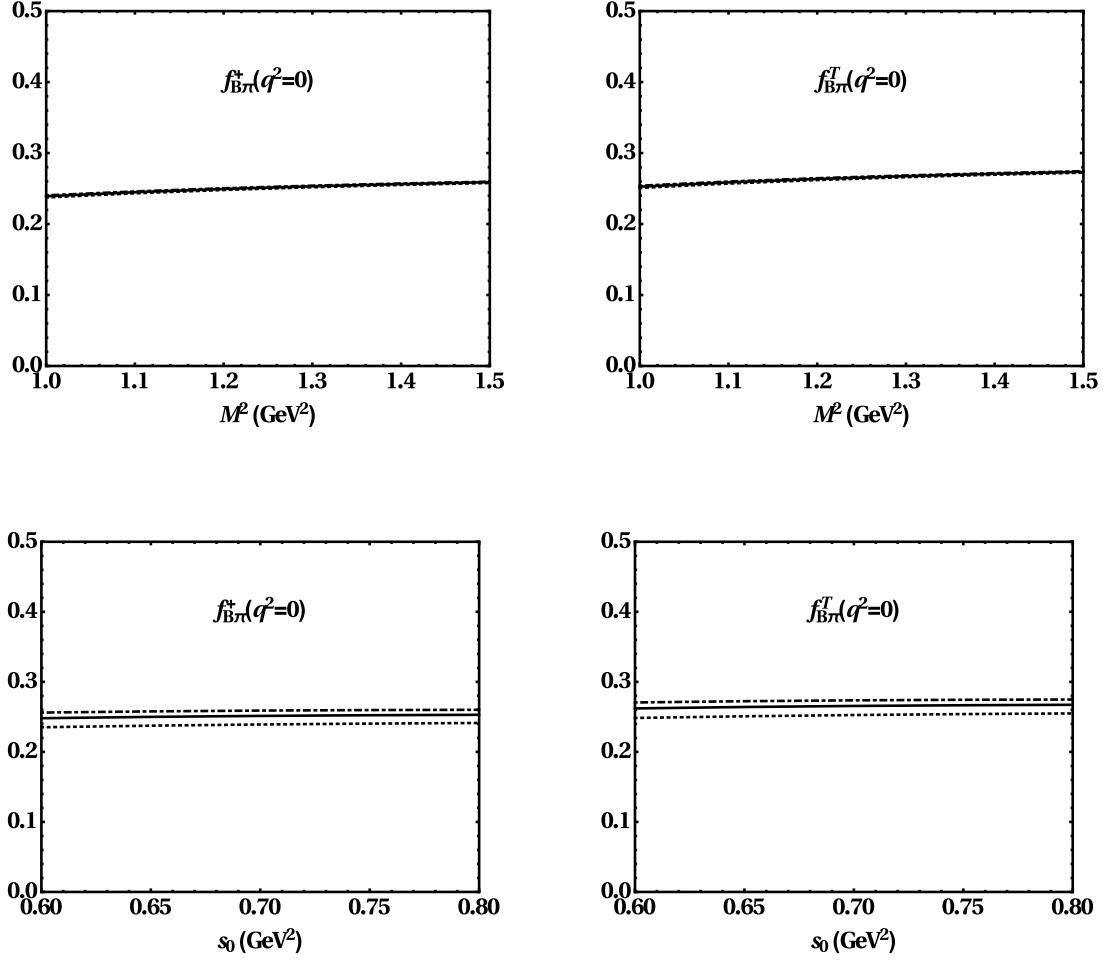


Figure 5: Borel parameter and effective threshold dependence of the form factors $f_{B\pi}^+(0)$ and $f_{B\pi}^T(0)$. The dotted, solid and dot-dashed curves correspond to $M^2 = 1.0\text{GeV}^2$, 1.25GeV^2 , 1.5GeV^2 (down panel) and $s_0 = 0.65, 0.70, 0.75$ (up panel), respectively.

vector form factors has been given in [3], and the tensor form factor has the similar form with $f^+(q^2)$ [26]

$$f_{B\pi}^T(q^2) = \frac{f_{B\pi}^T(0)}{1 - q^2/m_{B^*}^2} \left\{ 1 + \sum_{k=1}^{N-1} b_k^T \left(z(q^2, t_0)^k - z(0, t_0)^k - (-1)^{N-k} \frac{k}{N} \left[z(q^2, t_0)^N - z(0, t_0)^N \right] \right) \right\}, \quad (3.7)$$

where the expansion coefficients b_k can be determined by matching the computed $f_{B\pi}^T(q^2)$ at low q^2 onto Eq. (3.7). As the interval in z plane is constrained in a small region, it is reasonable to truncate the z -series at $N = 2$ in the practical calculation.

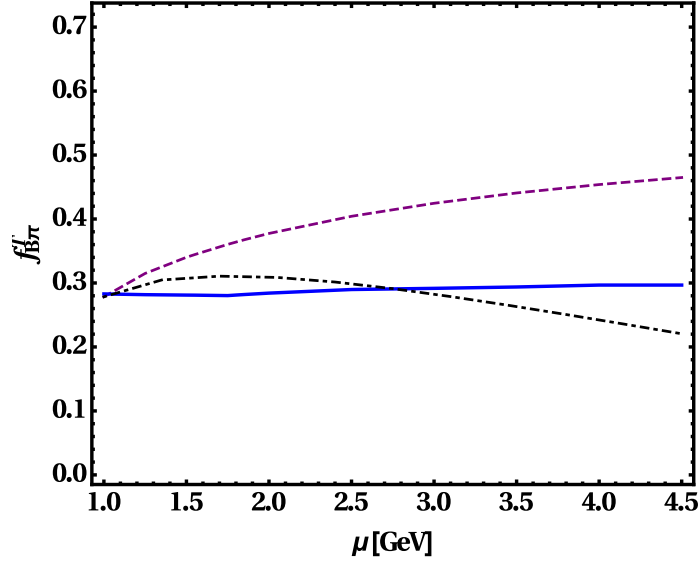


Figure 6: Scale dependence of the form factors. The purple dashed line represents RGE evolution only performed for the hard function and the B-meson decay constant, black dot-dashed line represents an addition evolution of inverse moment λ_B , blue solid line represents the complete RGE.

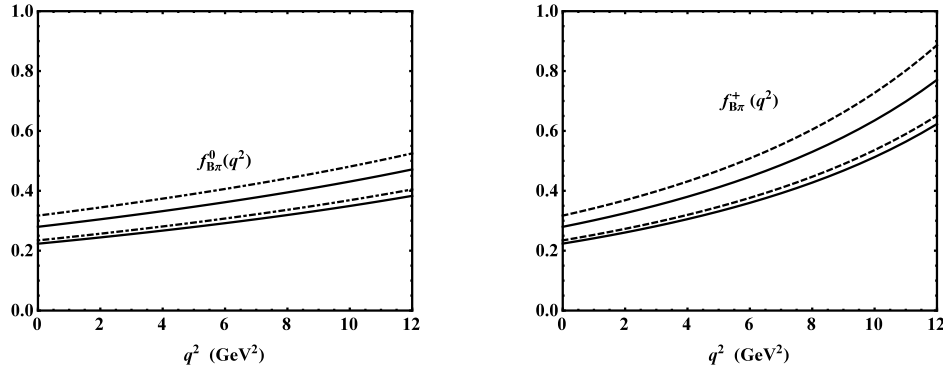


Figure 7: q^2 dependence of vector form factors $f_{B\pi}^0(q^2)$ and $f_{B\pi}^+(q^2)$. The region between the dashed curves indicates the uncertainties of form factor estimated in reference [8], while the region between the solid curves represents the results of ours.

In Fig. 7, the q^2 dependence of the two vector form factors $f_{B\pi}^{0,+}(q^2)$ are shown. They are computed from the LCSR with B -meson LCDAs at $q^2 < 8 \text{ GeV}^2$ with an extrapolation

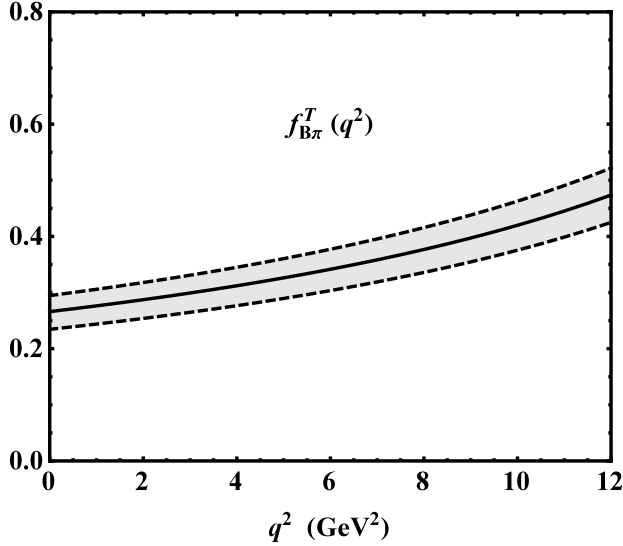


Figure 8: q^2 dependence of the tensor form factor. Solid curve represents center value, and region between the dashed curves indicates the estimated uncertainties.

to $q^2 = 12 \text{ GeV}^2$ using the z expansion. For a comparison, $f_{B\pi}^{0,+}(q^2)$ with incomplete RGE evolution are also presented. We can see from this diagram that after complete RGE evolution, the two form factors are slightly suppressed and the uncertainties are smaller, while the behavior of the q^2 dependence is merely unchanged. The q^2 dependence of the tensor form factor $f_{B\pi}^T(q^2)$ is also presented in Fig. 8, where a similar behavior like the vector case is shown. Furthermore, we provide the fitted $f_{B\pi}^+(q^2)$, $f_{B\pi}^T(0)$ and the slope parameter b_1, \tilde{b}_1, b_1^T corresponding to the form factors $f_{B\pi}^+(q^2)$, $f_{B\pi}^0(q^2)$, $f_{B\pi}^T(q^2)$ respectively in Table. 1. The uncertainties from different sources are also presented, and it is obvious that the inverse moment of the B -meson LCDAs is the most important. In Table. 1, the negligible uncertainties induced by variations of the remaining parameters are not shown, but are taken into account in the combined uncertainty.

At small recoil region, Lattice QCD is the most appropriate approach to study the heavy-to-light transition form factors. The Lattice data from HPQCD Collaboration [27] (blue squares), RBC/UKQCD Collaborations [28] (green triangles) and Fermilab/MILC [?] (red band) are displayed in Fig. 9, together with our fitted result. One can readily observe that at large q^2 our result is basically consistent with the lattice data for the form factor $f_{B\pi}^0(q^2)$, and slightly larger for the re-scaled form factor $(1 - q^2/m_B^2)f_{B\pi}^+(q^2)$.

4. CONCLUSION AND DISCUSSION

We computed the QCD corrections to $B \rightarrow \pi$ tensor form factor from the QCD LCSR

Parameter	default	ω_0	μ	μ_h	$\{M^2, s_0\}$
$f_{B\pi}^+(0)$	0.251	-0.023 $+0.023$	-0.000 $+0.003$	-0.002 $+0.003$	-0.012 $+0.008$
$f_{B\pi}^T(0)$	0.266	-0.026 $+0.023$	-0.000 $+0.002$	-0.005 $+0.003$	-0.013 $+0.008$
b_1	-4.02	-0.06 $+0.13$	-0.05 $+0.17$	-0.03 $+0.05$	-0.06 $+0.07$
\tilde{b}_1	-5.59	-0.09 $+0.16$	-0.05 $+0.04$	-0.00 $+0.03$	-0.10 $+0.11$
b_1^T	-0.18	-0.12 $+0.06$	-0.06 $+0.06$	-0.02 $+0.02$	-0.07 $+0.06$

Table 1: Z-parameter fitted values of the form factors $f_{B\pi}^+(0)$, $f_{B\pi}^T(0)$ ($f_{B\pi}^0(0)$ is not listed here because $f_{B\pi}^0(0) = f_{B\pi}^+(0)$) and of the slop parameters b_1 , \tilde{b}_1 and b_1^T . The notation “default” means that all the parameters are taken as the central values.

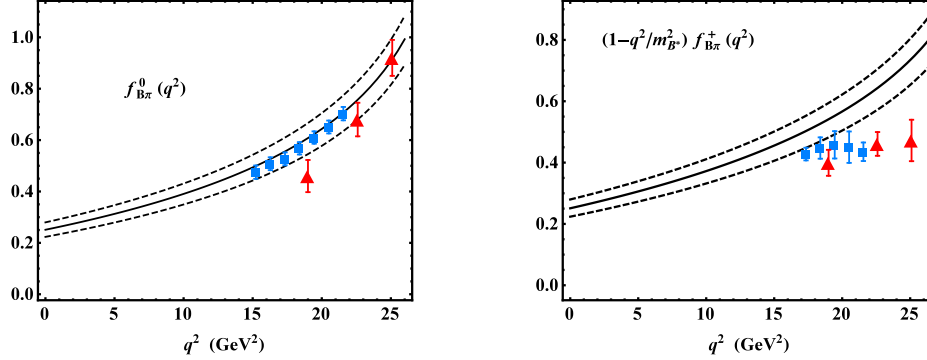


Figure 9: q^2 dependence of the form factor $f_{B\pi}^0(q^2)$, and the re-scaled form factor $(1 - q^2/m_B^2)f_{B\pi}^+(q^2)$ compared with lattice QCD results, taken from HPQCD Collaboration [27] (blue squares) and RBC/UKQCD Collaborations [28] (red triangles).

with B -meson LCDAs, following the same method in [8]. In this framework, the method of region is employed and contributions from different momentum regions are separated naturally. Precise soft cancellation guarantees the factorization theorem and the correlation functions are factorized into the hard function, the jet function and the wave function which corresponding to the hard, hard-collinear and soft region respectively. We obtained the one-loop level results of the hard function and the jet function. The former is consistent with the match coefficients between weak tensor current and SCET_I operators, and the latter reproduces the SCET sum rule results. Comparing with the vector form factors case, only small symmetry breaking effect appear in the hard function, in addition to the operator renormalization of the tensor current.

To eliminate the factorization scale dependence of the form factors, we carried out the complete RGE evolution to the factorized correlation functions, including the jet function

and the LCDAs, which are fixed at a special scale in [8]. The wave function, defined via the HQET heavy meson field, obeys the Lange-Neubert equation, which includes non-diagonal anomalous dimension. We followed the approach in [17], diagonalized the evolution equation and found the solution in the “dual” space. The same method was also applied to the evolution of the jet function. Combining the evolution of each part together, we obtained the final results of RGE improved form factors.

On the numerical side, we checked the behavior of each evolution kernel, and illustrated their cancellation effect. We examined the scale dependence of the form factors with the full RGE evolution, comparing with the previous results. We confirmed the almost scale independence of the form factors numerically. We then extrapolated the q^2 dependence of the form factors to the whole physical region using z -series expansion. It is of phenomenological importance, such as the tensor form factor can give important contribution to the FCNC precesses $B \rightarrow (\pi, K)l^+l^-$. Of course a complete study of these processes are far more complicated, and we left it for the future work. This work supplements the framework proposed in [8], and can be applied to various transition processes.

Acknowledgement

We are grateful to Y. M. Wang for useful discussions and comments. This work was supported in part by Natural Science Foundation of Shandong Province, China under Grant No. ZR2015AQ006 and by National Natural Science Foundation of China (Grants No. 11375208, No. 11521505, No. 11235005).

A. Jet function in the dual space

The jet function in the dual space is defined by

$$\begin{aligned} j^{(-)}\left(\frac{\mu_{hc}^2}{n \cdot p \hat{\omega}'}, \frac{\hat{\omega}'}{\bar{n} \cdot p}\right) &= \int_0^\infty \frac{d\omega}{\omega - \bar{n} \cdot p} J_0\left(2\sqrt{\frac{\omega}{\omega'}}\right) J^{(-)}\left(\frac{\mu^2}{n \cdot p \omega}, \frac{\omega}{\bar{n} \cdot p}\right) \\ &= \int_0^\infty \frac{d\eta}{1+\eta} J_0\left(2\sqrt{\frac{\eta}{\eta'}}\right) J^{(-)}(\eta, \mu), \end{aligned} \quad (\text{A.1})$$

where

$$\begin{aligned} J^{(-)}(\eta, \mu) &= 1 + \frac{\alpha_s C_F}{4\pi} \left[\ln^2 \frac{\mu^2}{-p^2} - 4 \ln(1+\eta) \ln \frac{\mu^2}{-p^2} \right. \\ &\quad \left. + 2 \ln^2(1+\eta) - \frac{\eta-2}{\eta} \ln(1+\eta) - \frac{\pi^2}{6} - 1 \right]. \end{aligned} \quad (\text{A.2})$$

Using the formula

$$\int_0^\infty \frac{x dx}{(x^2 + k^2)^{1-\lambda}} J_0(ax) = \frac{1}{\Gamma(1-\lambda)} \left(\frac{2k}{a}\right)^\lambda K_\lambda(ka), \quad (\text{A.3})$$

which is valid for $\lambda < 3/4$, and performing derivative with respect to λ , and taking the limit $\lambda \rightarrow 0$, we can get

$$\begin{aligned} \int_0^\infty \frac{d\eta}{1+\eta} J_0 \left(2\sqrt{\frac{\eta}{\eta'}} \right) &= 2K_0 \left(2\sqrt{\frac{1}{\eta'}} \right), \\ \int_0^\infty \frac{d\eta}{1+\eta} J_0 \left(2\sqrt{\frac{\eta}{\eta'}} \right) \ln(1+\eta) &= (\ln \eta' - 2\gamma_E) K_0 \left(2\sqrt{\frac{1}{\eta'}} \right), \\ \int_0^\infty \frac{d\eta}{1+\eta} J_0 \left(2\sqrt{\frac{\eta}{\eta'}} \right) \ln^2(1+\eta) &= \left[\frac{1}{2} \ln^2 \eta' - 2\gamma_E \ln \eta' + 2\gamma_E^2 - 2\psi'(1) \right] K_0 \left(2\sqrt{\frac{1}{\eta'}} \right) \\ &\quad + 2K_0^{(2,0)} \left(2\sqrt{\frac{1}{\eta'}} \right). \end{aligned} \quad (\text{A.4})$$

Another useful equation is

$$\int_0^\infty \frac{dx}{x} J_0(bx) \ln(1+x^2) dx = 2 \int_b^\infty \frac{K_0(\beta)}{\beta} d\beta. \quad (\text{A.5})$$

Taking the advantage of Eqs. (A.4) and (A.5), one can obtain Eq. (2.42).

B. Dispersion integrals

To obtain the final expression of the form factors, we need to extrapolate $\bar{n} \cdot p$ to physical region. For the consistency of our derivation, we must have

$$\int_0^\infty \frac{d\omega}{\omega - \Omega - i\epsilon} J_0 \left(2\sqrt{\frac{\omega}{\omega'}} \right) = 2K_0 \left(-2i\sqrt{\frac{\Omega}{\omega'}} \right). \quad (\text{B.1})$$

The above equation indicates that the single-value branch of the root and logarithmic function should be chosen to satisfy $-\Omega - i\epsilon = \Omega e^{-i\pi}$, with the branch cut being along the positive real axis. The following equation can be derived from Eq. (A.3)

$$\int_0^\infty \frac{d\omega}{\omega - \Omega - i\epsilon} \left(1 - \frac{\omega}{\Omega} \right)^\lambda J_0 \left(2\sqrt{\frac{\omega}{\omega'}} \right) = i\pi e^{i\lambda\pi} \left(\frac{\omega'}{\Omega} \right)^{\lambda/2} \frac{1}{\Gamma(1-\lambda)} H_\lambda^{(1)} \left(2\sqrt{\frac{\Omega}{\omega'}} \right). \quad (\text{B.2})$$

From which we obtain the following useful results:

$$\begin{aligned} \int_0^\infty \frac{d\omega}{\omega - \Omega - i\epsilon} \ln \left(1 - \frac{\omega}{\Omega} \right) J_0 \left(2\sqrt{\frac{\omega}{\omega'}} \right) &= -\frac{\pi^2}{2} J_0 \left(2\sqrt{\frac{\Omega}{\omega'}} \right) - \frac{\pi}{2} \ln \frac{\hat{\omega}'}{\Omega} N_0 \left(2\sqrt{\frac{\Omega}{\omega'}} \right) \\ &\quad - i \left[\frac{\pi^2}{2} N_0 \left(2\sqrt{\frac{\Omega}{\omega'}} \right) - \frac{\pi}{2} \ln \frac{\hat{\omega}'}{\Omega} J_0 \left(2\sqrt{\frac{\Omega}{\omega'}} \right) \right] \end{aligned} \quad (\text{B.3})$$

$$\begin{aligned} \int_0^\infty \frac{d\omega}{\omega - \Omega - i\epsilon} \ln^2 \left(1 - \frac{\omega}{\Omega} \right) J_0 \left(2\sqrt{\frac{\omega}{\omega'}} \right) &= \frac{i\pi}{2} \left(\frac{1}{2} \ln^2 \frac{\hat{\omega}'}{\Omega} + i\pi \ln \frac{\hat{\omega}'}{\Omega} - \frac{\pi^2}{3} \right) H_0^{(1)} \left(2\sqrt{\frac{\Omega}{\omega'}} \right) \\ &\quad + i\pi J_0^{(2,0)} \left(2\sqrt{\frac{\Omega}{\omega'}} \right) - \pi N_0^{(2,0)} \left(2\sqrt{\frac{\Omega}{\omega'}} \right). \end{aligned} \quad (\text{B.4})$$

Following a similar way, another useful result is also obtained

$$\int_0^\infty \frac{d\omega}{\omega} \ln\left(1 - \frac{\omega}{\Omega}\right) J_0\left(2\sqrt{\frac{\omega}{\omega'}}\right) = 2i\pi \int_{2\sqrt{\frac{\Omega}{\omega'}}}^\infty \frac{d\beta}{\beta} H_0^{(1)}(\beta). \quad (\text{B.5})$$

Taking the imaginary part of the above equation, we have

$$\text{Im} \int_0^\infty \frac{d\omega}{\omega} \ln\left(1 - \frac{\omega}{\Omega}\right) J_0\left(2\sqrt{\frac{\omega}{\omega'}}\right) = 2\pi \left[-\gamma_E + \frac{\Omega}{\omega'} {}_2F_3\left(1, 1; 2, 2, 2; -\frac{\Omega}{\omega'}\right) - \ln \frac{\Omega}{\omega'} \right]. \quad (\text{B.6})$$

Having all the above equations in hand, we get the final results in Eqs. (2.45) and (2.46).

References

- [1] V. M. Belyaev, A. Khodjamirian and R. Ruckl, Z. Phys. C **60**, 349 (1993) doi:10.1007/BF01474633 [hep-ph/9305348].
- [2] E. Bagan, P. Ball and V. M. Braun, Phys. Lett. B **417**, 154 (1998) doi:10.1016/S0370-2693(97)01371-3 [hep-ph/9709243].
- [3] A. Khodjamirian, T. Mannel, N. Offen and Y.-M. Wang, Phys. Rev. D **83** (2011) 094031 [arXiv:1103.2655 [hep-ph]].
- [4] A. Khodjamirian, T. Mannel and N. Offen, Phys. Lett. B **620** (2005) 52 [hep-ph/0504091].
- [5] A. Khodjamirian, T. Mannel and N. Offen, Phys. Rev. D **75** (2007) 054013 [hep-ph/0611193].
- [6] F. De Fazio, T. Feldmann and T. Hurth, Nucl. Phys. B **733** (2006) 1 [Nucl. Phys. B **800** (2008) 405] [hep-ph/0504088].
- [7] F. De Fazio, T. Feldmann and T. Hurth, JHEP **0802** (2008) 031 [arXiv:0711.3999 [hep-ph]].
- [8] Y. Wang and Y. Shen, Nucl. Phys. B **898** (2015) 563 [arXiv:1506.00667 [hep-ph]].
- [9] M. Beneke and V. A. Smirnov, Nucl. Phys. B **522** (1998) 321 [hep-ph/9711391].
- [10] C. W. Bauer, S. Fleming, D. Pirjol and I. W. Stewart, Phys. Rev. D **63** (2001) 114020 [hep-ph/0011336].
- [11] M. Beneke, A. P. Chapovsky, M. Diehl and T. Feldmann, Nucl. Phys. B **643**, 431 (2002) doi:10.1016/S0550-3213(02)00687-9 [hep-ph/0206152].
- [12] M. Beneke, Y. Kiyo and D. S. Yang, Nucl. Phys. B **692** (2004) 232 [hep-ph/0402241].
- [13] M. Beneke and D. S. Yang, Nucl. Phys. B **736** (2006) 34 [hep-ph/0508250].
- [14] A. G. Grozin and M. Neubert, Phys. Rev. D **55** (1997) 272 doi:10.1103/PhysRevD.55.272 [hep-ph/9607366].
- [15] M. Beneke and T. Feldmann, Nucl. Phys. B **592** (2001) 3 [hep-ph/0008255].
- [16] B. O. Lange and M. Neubert, Phys. Rev. Lett. **91** (2003) 102001 [hep-ph/0303082].
- [17] G. Bell, T. Feldmann, Y. M. Wang and M. W. Y. Yip, JHEP **1311** (2013) 191 [arXiv:1308.6114 [hep-ph]].
- [18] M. Beneke and T. Feldmann, Nucl. Phys. B **685** (2004) 249 [hep-ph/0311335].
- [19] S. Descotes-Genon and C. T. Sachrajda, Nucl. Phys. B **650** (2003) 356 [hep-ph/0209216].

- [20] Y. M. Wang and Y. L. Shen, JHEP **1602**, 179 (2016) [arXiv:1511.09036 [hep-ph]].
- [21] M. Beneke and J. Rohrwild, Eur. Phys. J. C **71** (2011) 1818 [arXiv:1110.3228 [hep-ph]].
- [22] V. M. Braun and A. N. Manashov, Phys. Lett. B **731** (2014) 316 [arXiv:1402.5822 [hep-ph]].
- [23] V. M. Braun, D. Y. Ivanov and G. P. Korchemsky, Phys. Rev. D **69** (2004) 034014 [hep-ph/0309330].
- [24] A. Heller *et al.* [Belle Collaboration], arXiv:1504.05831 [hep-ex].
- [25] M. Beneke and S. Jager, Nucl. Phys. B **768** (2007) 51 [hep-ph/0610322].
- [26] Z. H. Li, Z. G. Si, Y. Wang and N. Zhu, Nucl. Phys. B **900**, 198 (2015).
doi:10.1016/j.nuclphysb.2015.09.008
- [27] E. Dalgic, A. Gray, M. Wingate, C. T. H. Davies, G. P. Lepage and J. Shigemitsu, Phys. Rev. D **73** (2006) 074502 [Phys. Rev. D **75** (2007) 119906] [hep-lat/0601021].
- [28] J. M. Flynn, T. Izubuchi, T. Kawanai, C. Lehner, A. Soni, R. S. Van de Water and O. Witzel, Phys. Rev. D **91** (2015) 7, 074510 [arXiv:1501.05373 [hep-lat]].